ChemComm

Accepted Manuscript

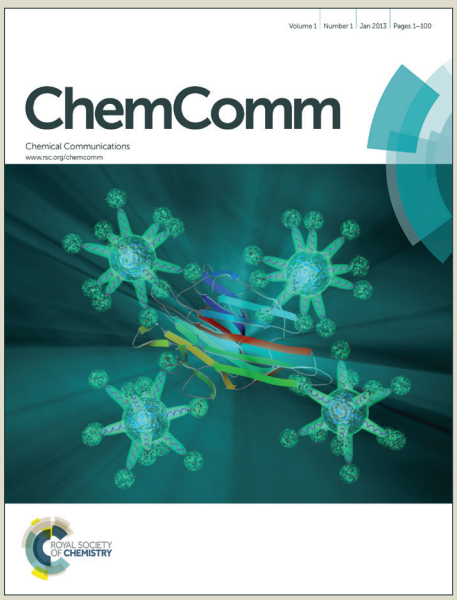

ROYAL SOCIETY OF CHEMISTRY

www.rsc.org/chemcomm

Chemical Communications

RSCPublishing

COMMUNICATION

Facile Synthesis of Nucleic Acid-Polymer Amphiphiles and their Self-assembly

Cite this: DOI: 10.1039/x0xx00000x

Fei Jia, Xueguang Lu, Xuyu Tan, and Ke Zhang*

Received 00th January 2012,
Accepted 00th January 2012

DOI: 10.1039/x0xx00000x

www.rsc.org/

A solid-phase synthesis for nucleic acid-polymer amphiphiles is developed. Using this strategy, several DNA-*b*-polymer amphiphiles are synthesized, and their self-assembly in aqueous solution is investigated. This general method can in principle be extended to nearly all polymers synthesized by atom transfer radical polymerization, to produce a variety of nucleic acid-polymer conjugates.

Nucleic acid-polymer amphiphiles (NAPAs) are a class of bioconjugate that is composed of a nucleic acid strand covalently attached to hydrophobic polymer.[1] These macromolecules undergo self-assembly in an aqueous solution, to yield morphologically and functionally interesting nanostructures with a high-density nucleic acid corona and a polymeric core.[2] Due to the tailorability of nucleic acid sequences and diverse properties of synthetic polymers, NAPA nanostructures have potential applications in many important areas, spanning biosensing,[3] drug delivery,[4] gene therapy,[5] and materials science.[6] Indeed, high-density nucleic acid nanostructures assembled from NAPAs exhibit several unusual properties associated with gold nanoparticle-DNA conjugates (termed spherical nucleic acids, or SNAs), which include the sharpening of the melting transition relative to free DNA strands, increased enzymatic stability against endonucleases, and higher binding affinity with complementary strands.[7] These unique properties make NAPA nanostructures attractive organic materials for biomedical applications. Despite these promises, however, there has been an absence of detailed investigation of the self-assembly of nucleic acid-polymer amphiphiles, in part due to a shortage of convenient synthetic access to these molecules.

Currently, solution-phase and solid-phase syntheses have been used to create DNA-*b*-polymer conjugates. Although hydrophilic polymers can be efficiently coupled with DNA strands in an aqueous environment, amphiphilic DNA-*b*-polymer conjugates are more difficult to achieve because of the lack of an appropriate solvent or solvent mixtures to simultaneously solubilize the hydrophobic polymer and the hydrophilic DNA.[8] DNA-surfactant complexes, to some extent, circumvent the issue, but challenging separation, low yields, and removal of surfactant can oftentimes be problematic.[9] On the other hand, solid-phase synthesis provides convenience in purification and is suitable for both hydrophilic and hydrophobic polymers.[10] The chemistry for solid-phase coupling must be carefully selected; it should be highly efficient to endure long coupling times, and be orthogonal to DNA synthesis. The functional groups required for conjugation should also be easily installed on both the DNA and the polymer in a regioselective fashion. The most commonly used reaction is the phosphoramidite chemistry, which provides a native phosphodiester linkage between the polymer and the nucleic acid. However, the reaction conditions are rather stringent, with small amounts of water leading to significantly reduced yields,[11] and installation of appropriate chain-end functional groups can be challenging.

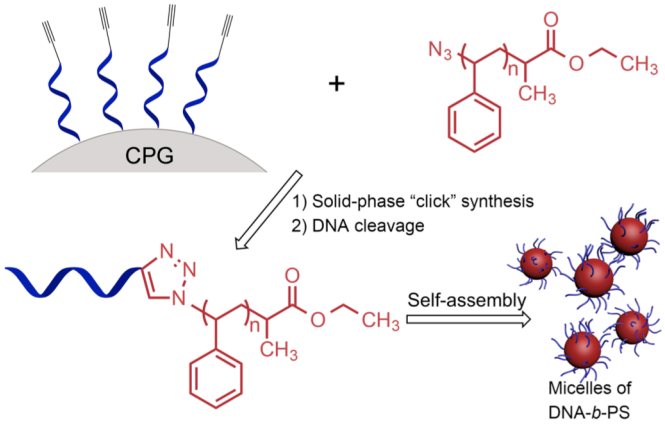

Scheme 1. Solid-phase "click" synthesis of DNA-*b*-polystyrene amphiphiles and their aqueous self-assembly.

Here, we developed an efficient route to achieve NAPAs on solid-supports (controlled pore glass, CPG) using copper-catalysed click chemistry and polymers synthesized *via* atom transfer radical polymerization (ATPR). ATRP is one of the most versatile and inexpensive free radical polymerization systems, which is capable of polymerizing a wide range of monomers including various styrenes, acrylates, as well as acrylonitrile, vinyl pyridine, and dienes.[12] ATRP polymers in general have low polydispersity indices and bear a halide moiety (typically a chloride or a bromide) at the ω chain-end of the polymer.[13] The halide group can be conveniently substituted by an azide anion,[14] which can undergo copper-catalysed click

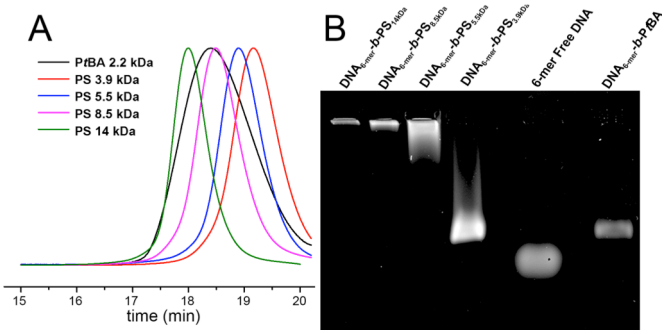

Figure 1. (A) Gel permeation chromatography (DMF) of all polymers used in NAPA synthesis. Broad P*t*BA MW distribution is due to solvent; *Cf.* Figure S1 for THF GPC chromatogram. (B) Agarose gel (0.5%) electrophoresis of free $DNA_{6\text{-mer}}$ and $DNA_{6\text{-mer}}$-*b*-polymer conjugates.

reaction with alkyne-modified oligonucleotides on the solid support (Scheme 1). Using this strategy, we successfully conjugated two hydrophobic polymers (poly(*t*-butyl acrylate), P*t*BA, and polystyrene, PS) of varying degrees of polymerization with DNA strands of three different lengths (6, 19, and 26 bases), with high yields. Having convenient access to a large set of NAPAs, we also conducted a preliminary investigation of the self-assembly of several PS NAPAs. Furthermore, we demonstrate that the nucleic acid component of the assembled structures remain hybridisable with complementary micelles, and higher-order assemblies of the NAPA micelles exhibit a sharp melting transition analogous to the assemblies of noble metal nanoparticle-DNA conjugates. The methodology herein enables the formation of NAPAs using nearly all ATRP polymers, and thus is a powerful tool to access a diverse range of NAPAs and their self-assembled nanostructures.

In a typical synthesis, the halide chain-end group of the polymer first reacts with sodium azide in dimethylformamide (DMF) to give azide-terminated polymers.[15] The azide substitution reaction generally shows high yields, even for high molecule weight polymers (nearly 100% as characterized by ^{1}H NMR and MALDI-TOF MS, Figures S2 and S3). Thereafter, the azide-terminated polymer is used for coupling with alkyne-terminated DNA on the CPG. Polymer chains lacking the azide chain-ends do not pose a complication to the coupling reaction, as they are removed by washing after the solid-phase reaction. The coupling is performed in dichloromethane at room temperature under nitrogen atmosphere, using copper iodide, acetic acid, and *N*,*N*-diisopropylethylamine as the catalyst system.[16] The alkyne modification for the oligonucleotide is commercially available, and can be achieved at either terminus or within the primary sequence of the oligonucleotide. After 8 h, unreacted polymers are removed by rinsing the CPG with solvents. The coupling with a hydrophobic polymer such as PS renders the surface of the CPG beads hydrophobic, as they no longer disperse well in aqueous solutions, which is indicative that the coupling reaction has succeeded. Next, ammonium hydroxide is used to cleave the DNA-*b*-polymer conjugate from the CPG beads, following typical DNA synthesis protocols. The conjugate is then purified and analysed by agarose gel electrophoresis.

Table 1. Yields of solid phase "click" synthesis of NAPAs as determined by band densitometry analysis.

DNA	P*t*BA 2.2 kDa	PS 3.9 kDa	PS 5.5 kDa	PS 8.5 kDa	PS 14 kDa
6-mer	99%	99%	99%	99%	99%
19-mer	86%	80%	77%	66%	66%
26-mer	80%	78%	74%	65%	56%

We tested a series of combinations of DNA lengths (6-, 19- and 26-mers) (DNA sequence see Table S1), polymers compositions (PS and P*t*BA), and polymer lengths (PS, M_n 5.5 kDa, 8.5 kDa, and 14 kDa; P*t*BA M_n 2.2 kDa; PDI 1.13-1.18, Table S2). Successful coupling of azide-modified PS and P*t*BA to the 6-mer DNA is confirmed by gel electrophoresis (Figure 1). The gel image of crude products without purification shows a single band of much higher molecular weight relative to the free DNA for each of the conjugates prepared, indicating that the yields for the coupling reactions are very high. As the length of the DNA or the polymer increases, a reduction in the yield was observed (Table 1). The reduction is due to a combination of DNA strands that failed to reach full length due to the non-unity yields of each synthetic step, and the strands with full length but failed to couple with the polymer. The reactions between of shorter polymers (2.2 kDa P*t*BA and 3.9 kDa PS) and a long oligonucleotide (26-mer DNA) have yields of *ca*. 80%, which is close to the yield of successful DNA synthesis itself, suggesting that the click coupling reaction likely remains nearly quantitative. The lowest yield is observed for the coupling between the 26-mer DNA and 14 kDa PS, which is 56%. Further increases of reaction times and azide-PS concentration do not result in higher conversions, indicating that the pore size of the CPG may be the limiting factor. Non-full-length DNA strands and DNA that failed to attach with polymers are removed by gel electrophoresis, and pure NAPAs are obtained by extraction from excised gel bands using a GenElute™ spin column.

Having obtained a large set of NAPAs, we next investigated the self-assembly of the DNA-*b*-PS NAPAs in an aqueous solution. Two methods were applied to achieve DNA-*b*-PS micelles: 1) micellization during the cleavage reaction by ammonium hydroxide, which liberates the NAPA from the CPG support, and 2) micellization by gradual addition of water to a DMF solution of the NAPAs. The first strategy mechanistically involves a two-step process: chain cleavage from solid support and the incorporation of chains into a micelle. Both steps are largely irreversible. For the first step, the aminolysis reaction of the succinoyl ester linkage between the CPG and the first deoxynucleotide is irreversible. For the second step, the exchange of the NAPA chains among micelles is very slow due to the large molecular weight and strong inter-chain interactions below the T_g of the polymer.[17] Thus, the micelles can be considered as a kinetic product, i.e. global equilibrium states are not reached. The second strategy, however, allows the NAPAs to stay in the equilibrium between micelles and free chains before moving to the micelle state, and thus the product should of a thermodynamic nature. Both methods yield micelles readily as demonstrated by gel electrophoresis, dynamic light scattering (DLS), and transmission electron microscopy (TEM). We systematically investigated the

nanostructures formed using the first strategy by all NAPAs from Table 1. A pseudo-phase behaviour was observed (Figure 2A). Spherical nanoparticles are formed with NAPAs with long DNA strands (19- and 26-mer) and short PS (3.9 kDa and 5.5 kDa). With increasing PS length, initially, an increase in the diameter of the spherical nanoparticles is observed (Figure 2C, F). Further increases of PS molecular weight result in rod-like structures with varying degrees of branching (Figures 2G, H and S4A-D). Conversely, using the second micellization method, all NAPA samples yielded spherical micelles, with a larger diameter than the cross-section diameter of the rod-like structure generated using the first method

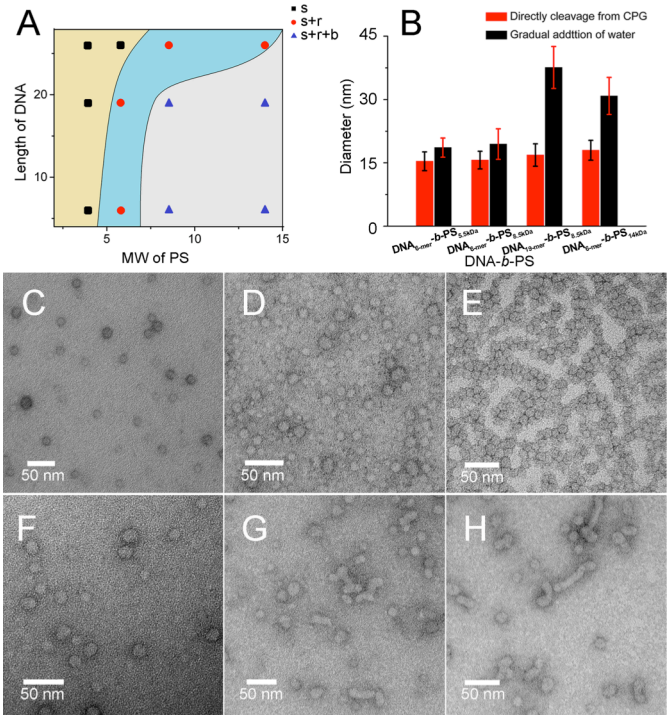

Figure 2. (A) Diagram of pseudo phase behaviour of NAPAs in kinetic micellization. S, r, and b: sphere, rod, and branch. (B) Dry-state diameter (for spheres) or cross-section diameter (for rods) of micelles generated using the first (red) and the second (black) micellization method. Sizes are determined by measuring at least 100 individual nanoparticles in several TEM images. (C-H) TEM images of kinetic micelles constructed from PS NAPAs, with uranyl acetate staining. From C to H: $DNA_{6\text{-mer}}$-*b*-$PS_{3.9kDa}$, $DNA_{19\text{-mer}}$-*b*-$PS_{3.9kDa}$, $DNA_{26\text{-mer}}$-*b*-$PS_{3.9kDa}$, $DNA_{6\text{-mer}}$-*b*-$PS_{5.5kDa}$, $DNA_{19\text{-mer}}$-*b*-$PS_{5.5kDa}$, and $DNA_{26\text{-mer}}$-*b*-$PS_{5.5kDa}$.

(Figures 2B and S4E-L). The prevalence of the spherical morphologies in the thermodynamic assemblies suggests that there exists strong repulsive interactions between the DNA strands even for NAPAs with short DNA and long PS segments (e.g. $DNA_{6\text{-mer}}$-*b*-PS_{14kDa}, Figure S4H),[18] which forces high interfacial curvatures between the hydrophilic corona and the hydrophobic core, leading to spherical micelles. In contrast, kinetic assemblies of NAPAs likely involve pre-collapsed PS chains, which cannot pack as compactly as mobile PS chains. Upon liberation from the solid support, the NAPAs form spherical micelles with a larger, albeit less packed cores. If the core:shell volume ratio is sufficiently large, then intermicellar aggregation can take place to minimize PS-water interfaces, which leads to rod-like structures with random branches. This hypothesis is corroborated by the thermal annealing reaction of the kinetically assembled rods at elevated temperatures (10 min at 99.5 °C, close to the T_g of PS of *ca*. 100 °C), which transformed rod-like nanostructures into spherical micelles (Figure 3).

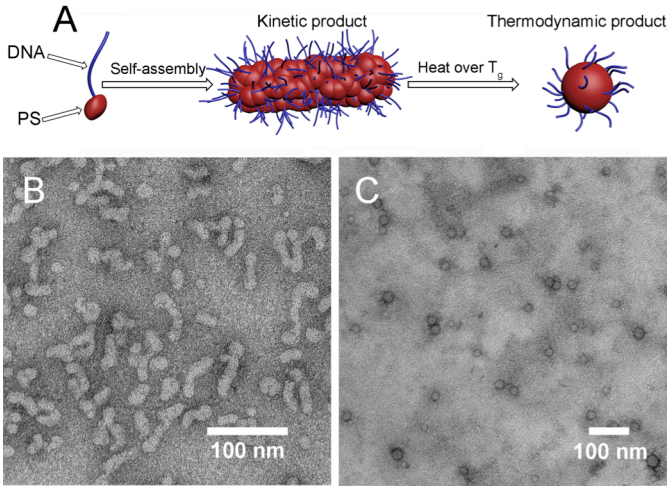

Figure 3. (A) Schematics for the kinetic micellization of $DNA_{6\text{-mer}}$-*b*-$PS_{8.5kDa}$ and subsequent thermal annealing, which caused a change in micelle morphology from rods (B) to spheres (C). TEM images are stained with uranyl acetate.

Next, we investigated whether the NAPA micelles can form higher-order assemblies *via* DNA hybridization, and whether the assemblies exhibit sharp melting transitions, which are characteristic for high-density nucleic acid nanostructures. We synthesized a pair of complementary NAPA micelles having a 19-mer DNA block and a 3.9 kDa PS block. The two micelles were suspended in 300 mM NaCl solution and then mixed at near-stoichiometric molar ratio (*ca.* 1.05:1, calculated from optical absorbance at 280 nm). The mixture

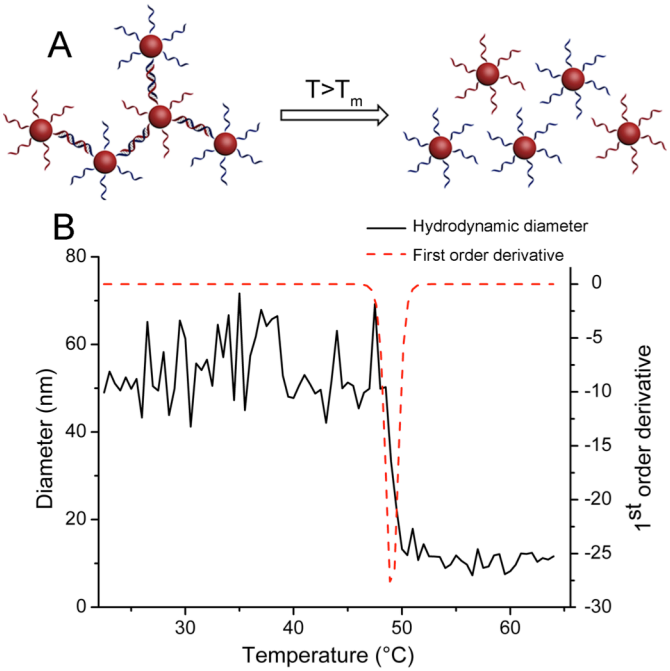

Figure 4. (A) Schematics for the thermal melting of an aggregate of a pair of complementary DNA-*b*-PS micelles. (B) DLS number-average hydrodynamic diameter of the aggregate as a function of temperature. Dashed red line show the first order derivative of a Boltzmann fitting (two iterations).

was annealed for 12 h at 45 °C, which is slightly below the melting temperature for the free DNA duplex (T_m = 48.5 °C). DLS was used to monitor the number-average hydrodynamic diameter and scattered light intensity as temperature is increased. A sharp transition was observed near the melting temperature of DNA duplex, during which the size decreased from *ca*. 56 nm to 12 nm. The full width at half maximum of the first-order derivative peak is *ca*. 1.6 °C, which is much sharper than the melting range of free DNA duplexes (*ca*. 20 °C) and is consistent with the sharp melting transitions of high-density nanoparticle-DNA conjugates with noble metal cores (SNAs). These results suggest that the NAPA nanostructures are structural and functional analogues of SNAs, and may exhibit similar properties.

In conclusion, we report a general and facile approach to prepare nucleic acid-polymer amphiphiles using ATRP polymers. The solid-phase "click" synthesis can be extended to hydrophilic polymers and other azide-terminated moieties. We have also investigated the kinetic and thermodynamic self-assembly of several DNA-*b*-PS amphiphiles, and examined the ability of the micelles to form higher-order supramolecular structures through DNA hybridization. It is anticipated that, with the incorporation of various types of functional, stimuli responsive, and/or biodegradable polymers into the DNA-*b*-polymer micelles, a broad range of bioactive materials can be accessed.

Notes and references

This material is based upon work supported by Northeastern University start-up fund and the National Science Foundation CAREER award under Award ID 1453255.

Department of Chemistry and Chemical Biology, Northeastern University, Boston, Massachusetts 02115, United States. E-mail: k.zhang@neu.edu

† Electronic Supplementary Information (ESI) available: [Experimental details and additional figures.]. See DOI: 10.1039/c000000x/

1 (a) K. J. Watson, S. Park, J. Im, S. T. Nguyen and C. A. Mirkin, *J. Am. Chem. Soc.,* 2001, **123**, 5592; (b) J. H. Jeong, S. W. Kim and T. G. Park, *Bioconjugate Chem.*, 2003, **14**, 473.

2 (a) M. P. Chien, A. M. Rush, M. P. Thompson and N. C. Gianneschi, *Angew. Chem. Int. Ed.*, 2010, **49**, 5076; (b) X. Lu, E. Watts, F. Jia, X. Tan and K. Zhang, *J. Am. Chem. Soc.,* 2014, **136**, 10214; (c) F. E. Alemdaroglu and A. Herrmann, *Org. Biomol. Chem.*, 2007, **5**, 1311; (d) T. R. Wilks, J. Bath, J. W. de Vries, J. E. Raymond, A. Herrmann, A. J. Turberfield, and R. K. O'Reilly, *ACS Nano*, 2013, **7**, 8561.

3 J. M. Gibbs, S. Park, D. R. Anderson, K. J. Watson, C. A. Mirkin and S. T. Nguyen, *J. Am. Chem. Soc.,* 2005, **127**, 1170.

4 (a) F. E. Alemdaroglu, N. C. Alemdaroglu, P. Langguth and A. Herrmann, *Adv. Mater.*, 2008, **20**, 899; (b) F. E. Alemdaroglu, N. C. Alemdaroglu, P. Langguth and A. Herrmann, *Macromol. Rapid Commun.*, 2008, **29**, 326; (c) S. S. Oh, B. F. Lee, F. A. Leibfarth, M. Eisenstein, M. J. Robb, N. A. Lynd, C. J. Hawker, and H. T. Soh, *J. Am. Chem. Soc.,* 2014, **136**, 15010

5 (a) T. Chen, C. S. Wu, E. Jimenez, Z. Zhu, J. G. Dajac, M. You, D. Han, X. Zhang and W. Tan, *Angew. Chem. Int. Ed.*, 2013, **52**, 2012; (b) S. Cogoi, M. Ballico, G. M. Bonora and L. E. Xodo, *Cancer Gene Ther.*, 2004, **11**, 465; (c) J. H. Jeong and T. G. Park, *Bioconjugate Chem.*, 2001, **12**, 917.

6 M. Kwak, J. Gao, D. K. Prusty, A. J. Musser, V. A. Markov, N. Tombros, M. C. Stuart, W. R. Browne, E. J. Boekema, G. ten Brinke, H. T. Jonkman, B. J. van Wees, M. A. Loi and A. Herrmann, *Angew. Chem. Int. Ed.*, 2011, **50**, 3206.

7 J. I. Cutler, E. Auyeung and C. A. Mirkin, *J. Am. Chem. Soc.,* 2012, **134**, 1376.

8 (a) K. Lee, L. K. Povlich and J. Kim, *Adv. Func. Mater.*, 2007, **17**, 2580; (b) J. H. Jeong, S. H. Kim, S. W. Kim and T. G. Park, *Bioconjugate. Chem.*, 2005, **16**, 1034.

9 K. Liu, L. Zheng, Q. Liu, J. W. de Vries, J. Y. Gerasimov and A. Herrmann, *J. Am. Chem. Soc.,* 2014, **136**, 14255.

10 (a) Z. Li, Y. Zhang, P. Fullhart and C. A. Mirkin, *Nano Lett.*, 2004, **4**, 1055; (b) F. E. Alemdaroglu, K. Ding, R. Berger and A. Herrmann, *Angew. Chem. Int. Ed.*, 2006, **45**, 4206; (c) F. Teixeira, Jr., P. Rigler and C. Vebert-Nardin, *Chem. Commun.*, 2007, 1130.

11 (a) D. C. Capaldi, A. N. Scozzari, D. L. Cole and V. T. Ravikumar, *Org. Process. Res. Dev.*, 1999, **4**, 485; (b) M. H. Caruthers, A. D. Barone, S. L. Beaucage, D. R. Dodds, E. F. Fisher, L. J. McBride, M. Matteucci, Z. Stabinsky abd J. -Y. Tang, *Meth. Enzymol.*, 1987, **154**, 287.

12 K. Matyjaszewski, *Macromolecules*, 2012, **45**, 4015.

13 K. Matyjaszewski and J. Xia, *Chem. Rev.*, 2001, **101**, 2921.

14 T. P. Veerle Coessens and Krzysztof Matyjaszewski, *Prog. Polym. Sci.*, 2001, **26**, 337.

15 J. F. Lutz, H. G. Börner and K. Weichenhan, *Macromol. Rapid Commun.*, 2005, **26**, 514.

16 C. Shao, X. Wang, Q. Zhang, S. Luo, J. Zhao and Y. Hu, *J. Org. Chem.*, 2011, **76**, 6832.

17 (a) J. H. Zhu, S. Y. Zhang, K. Zhang, X. J. Wang, J. W. Mays, K. L. Wooley and D. J. Pochan, *Nat. Commun.*, 2013, **4**, 84; (b) H. G. Cui, Z. Y. Chen, S. Zhong, K. L. Wooley and D. J. Pochan, *Science*, 2007, **317**, 647; (c) Y. Li, E. Themistou, J. Zou, B. P. Das, M. Tsianou, and C. Cheng, *ACS Macro Lett.*, 2012 ,**1**, 52

18 (a) S. J. Hurst, A. K. R. Lytton-Jean and C. A. Mirkin, *Abstr. Pap. Am. Chem. S.*, 2007, **233**; (b) A. G. Cheetham, P. Zhang, Y. Lin, L. L. Lock, and H. Cui, *J. Am. Chem. Soc.,* 2013, **135**, 2907.